

2009-06-30

## Recovery Time Scales In A Reversed-Biased Quantum Dot Absorber

T. Piwonski

*Department of Physical Sciences, Cork Institute of Technology*

Gillian Madden

*Department of Physical Sciences, Cork Institute of Technology*

Jaroslav Pulka

*Department of Physical Sciences, Cork Institute of Technology*

Guillaume Huyet

*Department of Physical Sciences, Cork Institute of Technology*

Et. al.

Follow this and additional works at: <https://sword.cit.ie/dptphysciart>



Part of the [Physical Sciences and Mathematics Commons](#)

---

### Recommended Citation

Viktorov, E.A. et al., 2009. Recovery time scales in a reversed-biased quantum dot absorber. *Applied Physics Letters*, 94(26), p.263502. Available at: <http://dx.doi.org/10.1063/1.3159838>.

This Article is brought to you for free and open access by the Physical Sciences at SWORD - South West Open Research Deposit. It has been accepted for inclusion in Physical Sciences Publications by an authorized administrator of SWORD - South West Open Research Deposit. For more information, please contact [sword@cit.ie](mailto:sword@cit.ie).

## Recovery time scales in a reversed-biased quantum dot absorber

Evgeny A. Viktorov,<sup>1</sup> Thomas Erneux,<sup>1</sup> Paul Mandel,<sup>1,a)</sup> Tomasz Piwonski,<sup>2</sup> Gillian Madden,<sup>2</sup> Jaroslaw Pulka,<sup>2</sup> Guillaume Huyet,<sup>2</sup> and John Houlihan<sup>3</sup>

<sup>1</sup>*Optique Nonlinéaire Théorique, Université Libre de Bruxelles, Campus Plaine, Code Postal 231, 1050 Bruxelles, Belgium*

<sup>2</sup>*Tyndall National Institute, Cork, Ireland and Department of Applied Physics, Cork Institute of Technology, Ireland*

<sup>3</sup>*Department of Computing, Maths and Physics, Waterford Institute of Technology, Waterford, Ireland*

(Received 14 May 2009; accepted 8 June 2009; published online 30 June 2009)

The nonlinear recovery of quantum dot based reverse-biased waveguide absorbers is investigated both experimentally and analytically. We show that the recovery dynamics consists of a fast initial layer followed by a relatively slow decay. The fast recovery stage is completely determined by the intradot properties, while the slow stage depends on the escape from the dot to the wetting layer.

© 2009 American Institute of Physics. [DOI: 10.1063/1.3159838]

The physical properties of quantum dot (QD) based optical devices has been studied intensively in recent years<sup>1</sup> with particular attention given on their absorption properties. This has led to their use as monolithic mode-locked lasers,<sup>2</sup> electroabsorption modulators<sup>3</sup> and saturable absorber mirrors.<sup>4</sup> To explore the underlying carrier dynamics, time-resolved pump-probe spectroscopy has been applied to such QD structures in order to explain the nature of tunneling processes at high reverse bias voltages,<sup>5</sup> to demonstrate the electroabsorption properties of a bilayer QD waveguide,<sup>6</sup> and to illustrate the importance of Auger processes when the dots excited state (ES) is initially populated.<sup>7</sup> In this letter, we investigate the nonlinear recovery of QD based reverse-biased waveguide absorbers experimentally, analytically, and numerically. Our study highlights the role of the capture and escape processes in the formation of a fast initial layer followed by a relatively slow relaxation. We show that the fast stage is completely determined by the intradot relaxation properties while the slow recovery stage depends on the escape from the dot to the wetting layer.

Our experiment uses time-resolved pump probe spectroscopy to study the nonlinear recovery of QD based reversed-biased waveguide absorbers as a function of reverse bias. The QD waveguide absorber was 1 mm long had a 4  $\mu\text{m}$  width ridges together with tilted antireflection coated facets. It was fabricated from material that included six stacks of InAs/GaAs QDs in a dots-in-a-well structure, grown by Zia, Inc. (see Ref. 8 for further details of the material and experimental technique). Ground state (GS) and ES appear at 1320 and 1250 nm, respectively. The pump-probe differential transmission was measured at the dots' GS using a heterodyne detection technique. In reverse bias, the saturation fluence varied from  $\sim 0.1 \text{ J/m}^2$  at 0 V to  $0.6 \text{ J/m}^2$  at 9 V.

Pulses of about 600 fs width at either 1320 or 1250 nm were obtained from a titanium-sapphire pumped, optical parametric oscillator and split into three beams: reference, pump, and probe. After propagation through the waveguide absorber with suitable delays, the probe and reference beams were overlapped on a detector. The amplitude of the difference frequency was detected using a high frequency lock-in

amplifier. This signal is proportional to the differential transmission  $\Delta T$  of a probe pulse at the same wavelength as the pump. The resulting data are normalized to the maximum differential transmission at zero reverse bias  $T_0$  and therefore represented by  $\Delta T/T_0$ .

Figure 1 displays such differential transmission dynamics for reverse bias voltages ranging for 0–2 V. As outlined in our previous paper,<sup>7</sup> the experimental time traces can be classified into two groups depending on the reverse bias voltage. The recovery dynamics in the low voltage (0–4 V) group exhibits a two-stage recovery. During the fast initial stage ( $\approx 2$  ps) the response to the pump quickly relaxes to approximately half of its original value. This fast evolution does not significantly depend on the reverse bias. On the other hand, the slow ( $> 10$  ps) stage is voltage-dependent and changes in the range of 10–100 ps. For higher (5–9 V) reverse voltages, the recovery consists of only one fast stage ( $< 10$  ps) and the slow stage cannot be identified.

The QD carrier dynamics for the absorber is described by the occupation probabilities  $\rho_g$  and  $\rho_e$  of the GS and the first ES of a dot, respectively. They satisfy the following equations:

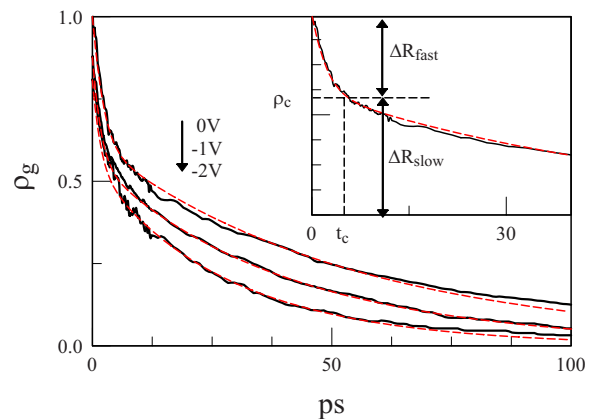


FIG. 1. (Color online) Experimental GS carrier relaxation for different reverse biased voltages (black) and fitting (red) with Eqs. (1) and (2): (a) 0 V,  $\tau_w=18$  ps; (b) 1 V,  $\tau_w=12$  ps; and (c) 2 V,  $\tau_w=8$  ps. The other fitting parameters are:  $\tau_{\text{cap}}=2$  ps and  $\tau_{\text{esc}}=10$  ps. The inset illustrates  $t_c$ ,  $\rho_c$ ,  $\Delta R_{\text{slow}}$ , and  $\Delta R_{\text{fast}}$  which are introduced in the text.

<sup>a)</sup>Electronic mail: pmandel@ulb.ac.be.

$$\frac{d\rho_g}{dt} = -\tau^{-1}\rho_g + 2\tau_{\text{cap}}^{-1}\rho_e(1-\rho_g) - 2\tau_{\text{esc}}^{-1}\rho_g(1-\rho_e), \quad (1)$$

$$\frac{d\rho_e}{dt} = -\tau_w^{-1}\rho_e - \tau_{\text{cap}}^{-1}\rho_e(1-\rho_g) + \tau_{\text{esc}}^{-1}\rho_g(1-\rho_e), \quad (2)$$

where  $1-\rho_{g,e}$  is the Pauli blocking factor<sup>9</sup> and  $\tau_{\text{cap}}^{-1}$  ( $\tau_{\text{esc}}^{-1}$ ) is the carrier capture (escape) rates. We assume that  $\rho_g(0)=\rho_0 \leq 1$  depends on the reverse bias. We also assume that  $\rho_e(0)=0$  meaning that initially there are no free carriers in the ES. The term  $\tau_{\text{cap}}^{-1}\rho_e(1-\rho_g)$  describes recapture by the GS. It is linearly proportional to the population of the ES and corresponds to a phonon-assisted interaction. The factor 2 in Eq. (1) accounts for the spin degeneracy in the QD energy levels.  $\tau \approx 1$  ns is the carrier recombination time in the dots. We assume that the reverse bias conditions do not allow capture of carriers from the wetting layer and model the relaxation from the ES to the wetting layer by the linear term  $\tau_w^{-1}\rho_e$ . The parameter  $\tau_w^{-1}$  is the carrier escape rate from the ES to the wetting layer and it strongly depends on the reverse bias.

The parameters  $\tau_{\text{cap}}$ ,  $\tau_{\text{esc}}$ , and  $\tau_w$  determine the time-dependent recovery of the QD absorber. In the low voltage range (0–4 V), we find that the variations of  $\tau_{\text{cap}}$  and  $\tau_{\text{esc}}$  with respect to the applied voltage  $V$  are negligible. The dynamics of GS transmission can then be analyzed by only taking into account the voltage dependence of  $\tau_w$ .

Comparative fits between the experimental results and the numerical solution of Eqs. (1) and (2) are shown in Fig. 1 for the 0–2 V range. The fits show a very good agreement with the experimental data for  $\tau_{\text{cap}}=2$  ps and  $\tau_{\text{esc}}=10$  ps. As pointed out in Ref. 7,  $\tau_w=\tau_w(V)$  can be described as  $\tau_w=\tau_{w0} \exp(-|V/V_0|)$ , where  $\tau_{w0}=18$  ps and  $V_0 \approx -2$  V. The same dependence with  $\tau_{w0} \approx 20$  ps was used to describe the recovery of quantum well based structures<sup>10</sup> and used in the modeling.<sup>11</sup> The exponential dependence on the applied voltage has been linked to a thermally activated rate process as introduced in Ref. 12. For QD structures, a similar exponential variation of thermionic emission time with voltage  $V_0=-3.8$  V was considered in Ref. 5 and was related to an expected drop in barrier height with the voltage.

The low voltage recovery dynamics clearly indicates a two-stage evolution. After a fast initial stage, the solution slowly decays starting near  $t=t_c$ , as shown in Figs. 1 and 2. Our main objective is to identify the relevant time scales for both the fast and slow stages. First, in Eq. (1), we neglect  $-\tau^{-1}\rho_g$  assuming that it remains small compared to the last term. Second, we note that  $d\rho_g/dt + 2d\rho_e/dt = -2\tau_w^{-1}\rho_e$  is linear which motivates introducing the new variable  $x \equiv \rho_g + 2\rho_e$ . After reformulating Eqs. (1) and (2) in terms of  $x$  and  $y \equiv \rho_e$ , we insert the dimensionless time  $s \equiv t/\tau_w$  and obtain

$$\frac{dx}{ds} = -2y, \quad (3)$$

$$\frac{dy}{ds} = -y - Cy(1-x+2y) + R(x-2y)(1-y), \quad (4)$$

where  $C \equiv \tau_w/\tau_{\text{cap}}$  and  $R \equiv \tau_w/\tau_{\text{esc}}$ . The initial conditions for  $x$  and  $y$  are  $x(0)=\rho_0$  and  $y(0)=0$ . Equations (3) and (4) cannot be solved exactly and we shall take advantage of the large value of  $C$  (for  $\tau_w=18$  ps,  $C=9$ , and  $R=1.8$ ). To this end, we first need to scale  $R$  with respect to  $C$ . The best

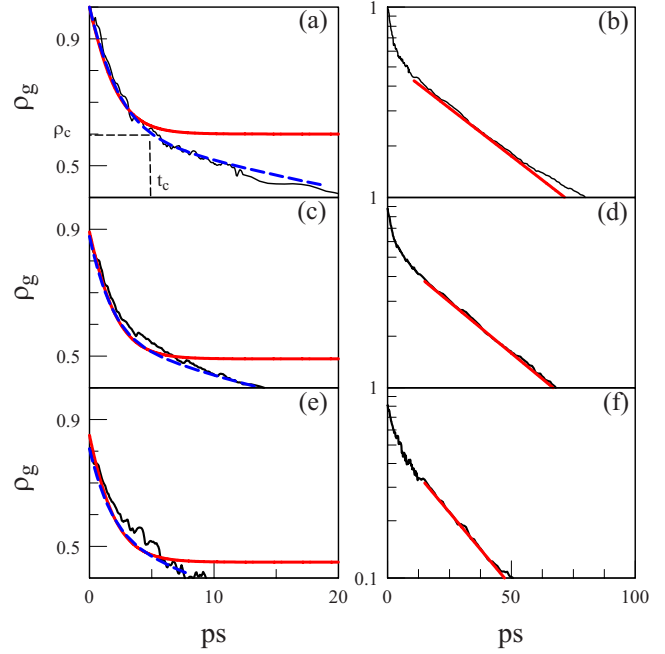


FIG. 2. (Color online) Experimental GS carrier relaxations (black), fitting with Eqs. (1) and (2) (blue), and fitting (red) with: [(a), (c), and (e)] Eq. (5) for the fast recovery stage; [(b), (d), and (f)] Eq. (8) for the slow recovery stage. The fitting parameters were: [(a) and (b)]  $\tau_w=18$  ps; [(c) and (d)]  $\tau_w=12$  ps; and [(e) and (f)]  $\tau_w=8$  ps. The other parameters are the same as in Fig. 1.

approximation we have found is obtained by scaling  $R$  as  $R=C\varepsilon$ , where  $\varepsilon=\tau_{\text{cap}}/\tau_{\text{esc}} \ll 1$ . The two-stage recovery then consist of a fast stage or initial layer ( $\Delta s \sim 1/C$  which is  $\Delta t \sim \tau_{\text{cap}}$ ) followed by a slow almost exponential decay ( $\Delta s \sim 1$  which means that the decay is determined by  $\tau_w$ ). It is worth to emphasize that the size of the initial layer is of the order of  $\tau_{\text{cap}}$ , and not of the order of  $\tau_{\text{esc}}$  as would be assumed intuitively.

To determine the initial layer solution, we introduce the fast time  $S \equiv Cs$  into Eqs. (3) and (4). The leading order problem for  $C$  large leads to  $dx/dS=0$ , implying  $x=\rho_0$ , and a simpler equation for  $y$  that can be integrated. Knowing  $y(S)$ , we determine  $\rho_g(t)=\rho_0-2y(t)$  and find

$$\rho_g(t) = \rho_0 - 2 \frac{\rho_+ [1 - \exp(-t/\tau_f)]}{1 - \rho_+/\rho_- \exp(-t/\tau_f)}, \quad (5)$$

where

$$\tau_f^{-1} \equiv \alpha C / \tau_w$$

with  $\alpha \equiv \sqrt{[1-\rho_0 + \varepsilon(2+\rho_0)]^2 + 8(1-\varepsilon)\varepsilon\rho_0}$  and  $\rho_{\pm} = [-(1-\rho_0 + \varepsilon(2+\rho_0)) \pm \alpha]/(4(1-\varepsilon))$ . This solution was used for the fits in Fig. 2. In our fits,  $\rho_0$  is close to 1 and  $\varepsilon \ll 1$ . Considering then both  $1-\rho_0$  and  $\varepsilon$  as small,  $\tau_f$  reduces to the simple expression

$$\tau_f \approx \sqrt{\tau_{\text{esc}}\tau_{\text{cap}}/8}. \quad (6)$$

The fast initial layer time  $\tau_f$  does not depend on  $\tau_w$ , in first approximation, and is only determined by the intradot transition properties. The initial layer approximation ends as  $t/\tau_f \rightarrow \infty$  when  $\rho_g \rightarrow \rho_c$  where

$$\rho_c \equiv \rho_0 - 2\rho_+ \quad (7)$$

We define the critical time  $t_c$  where the slow evolution starts by the condition  $\rho(t_c) = \rho_c$  [see Figs. 1 and 2(a)].

The function (5) is highly nonlinear and cannot be reduced to a single exponential. As a result, the value  $\tau_f = 1.58$  ps provided by Eq. (6) is different from the value obtained by a simple exponential fitting  $\tau_f \sim 2.4$  ps. If the dots have a large initial population ( $\rho_0 \approx 1$ ), the parameters  $\tau_f$  and  $y_{\pm}$  weakly depend on the initial conditions. However, if  $\rho_0 < 1$ , we need to take into account its effect on both  $\tau_f$  and  $\rho_{\pm}$ . We have considered the low voltage case. However, if the voltage is increased, the capture time to the GS  $\tau_{\text{cap}}$  may become comparable to the escape time to the well  $\tau_w$  and our basic assumption that  $\tau_{\text{cap}} \ll \tau_w$  is no more valid.

The fast transition layer is followed by a slow stage. From Eqs. (3) and (4), we now find that the leading order problem for  $C$ , large is given by Eq. (3) and, from Eq. (4), a nonlinear algebraic equation relating  $x$  and  $y$ . The latter provides  $x$  as a function of  $y$  and, using Eq. (3), we formulate a single equation for  $y$  that can be integrated. The solution is in the implicit form  $s = s(y)$  and the integration constant is determined by matching with the initial layer solution. This solution shows a gradual evolution to a pure exponential decay in the slow stage given by

$$\rho_g \sim \exp(-t/\tau_s), \quad (8)$$

where

$$\tau_s \equiv \tau_w \left( 1 + \frac{\tau_{\text{esc}}}{2\tau_{\text{cap}}} \right). \quad (9)$$

The expression (9) leads to the value  $\tau_s \approx 30\text{--}70$  ps and depends on  $\tau_w$ . This means that a relatively large recovery range  $t \gg t_c$  is needed to fit the experimental data. Note that  $\tau_s$  is directly proportional to the escape times  $\tau_w$  and  $\tau_{\text{esc}}$ . We emphasize that we considered the case of slow carrier recombination with  $\tau \approx 1$  ns and that the two-stage recovery dynamics does not depend on  $\tau$ , in first approximation. However, a faster recombination process could significantly change the slow recovery stage. In our analysis, Eq. (3) will admit an additional term but Eq. (2) will remain unchanged. Comparisons between the experimental data and the analytical approximations (5) and (8) are shown in Fig. 2 and indicate a very good agreement.

We next wish to analyze the ratio of the fast and slow recovery stages  $\Delta R_{\text{slow}}/\Delta R_{\text{fast}}$  or the relative modulation strength of the absorber.<sup>4</sup>  $\Delta R_{\text{slow}}$  and  $\Delta R_{\text{fast}}$  are defined by the deviations  $\Delta R_{\text{slow}} \equiv \rho_c$  and  $\Delta R_{\text{fast}} \equiv \rho_0 - \rho_c$ , respectively (see the inset in Fig. 1). For optimization of a fast saturable absorber, a small ratio  $\Delta R_{\text{slow}}/\Delta R_{\text{fast}} \ll 1$  is desirable. Using Eq. (7), we find that  $\Delta R_{\text{slow}}/\Delta R_{\text{fast}} = \rho_0/(2\rho_+) - 1$  only depends on the relative rate  $\varepsilon = \tau_{\text{cap}}/\tau_{\text{esc}}$  of the energy exchange between the GS and ES and on the initial condition  $\rho_0$ . For  $\rho_0 \approx 1$  and  $\varepsilon$  small,  $\Delta R_{\text{slow}}/\Delta R_{\text{fast}} \approx 1/\sqrt{2\tau_{\text{cap}}/\tau_{\text{esc}}} - 1$ . The increase of

$\tau_{\text{cap}}/\tau_{\text{esc}}$  corresponds to a decrease of  $\Delta R_{\text{slow}}/\Delta R_{\text{fast}}$  and therefore the modulation strength can be tunable with temperature.

To complete the analysis, we note that in the higher voltage range (5–9 V), the escape to the wetting layer becomes very fast ( $\tau_w \leq 3$  ps), which quickly leads to  $\rho_c(t) \approx 0$ . It means the disappearance of the slow recovery stage and the GS relaxation allows a linear approximation.<sup>7</sup> This linear approximation has been recently verified.<sup>5</sup>

In summary, we analyzed the recovery time scales of a reversed bias waveguide absorber. In the low voltage range, this recovery consists of a fast initial layer followed by a slow relaxation. The time scale of the fast stage admits the approximation (6) ( $\tau_f \approx 1.58$  ps) and is independent of voltage. The time scale of the slow stage depends on voltage and its approximation is given by Eq. (9) leading to  $\tau_s \approx 30\text{--}70$  ps. We also found that the relative contribution of the slow stage in terms of  $\rho_g$  can be reduced by increasing the relative rate  $\tau_{\text{cap}}/\tau_{\text{esc}}$ . This could be achieved by either controlling growth parameters and/or the operating temperature. This may become important in applications that preclude operation in the tunneling dominated regime that occurs at high reverse bias.

This study has been supported by Science Foundation Ireland under the Contract No. 07/IN.1/I929, the Tyndall National Access Programme, the INSPIRE programme funded by the Irish Government's Programme for Research in Third Level Institutions, Cycle 4, National Development Plan 2007-2013, and the Institutes of Technology Ireland funding under the Technological Sector Research Strand 1 programme. The authors in Bruxelles acknowledge support of the Fonds National de la Recherche Scientifique (Belgium).

<sup>1</sup>D. Bimberg, *J. Phys. D* **38**, 2055 (2005).

<sup>2</sup>M. G. Thompson, C. Marinelli, Y. Chu, R. L. Sellin, R. V. Penty, L. H. White, M. Van Der Poel, D. Birkedal, J. Hvam, V. M. Ustinov, M. Lammlin, and D. Bimberg, *Semiconductor Laser Conference, 2004. Conference Digest. 2004 IEEE 19th International*, 2004 (unpublished), pp. 53–54.

<sup>3</sup>Y. Chu, M. G. Thompson, R. V. Penty, I. H. White, and A. R. Kovsh, *OSA Technical Digest CLEO/QELS*, 2007 (unpublished), p. CMP4.

<sup>4</sup>D. J. H. C. Maas, A. R. Bellancourt, M. Hoffman, B. Rudin, Y. Barbarin, M. Golling, T. Sudmeyer, and U. Keller, *Opt. Express* **16**, 18646 (2008).

<sup>5</sup>D. B. Malins, A. Gomez-Iglesias, S. J. White, W. Sibbett, A. Miller, and E. U. Rafailov, *Appl. Phys. Lett.* **89**, 171111 (2006).

<sup>6</sup>D. Malins, A. Gomez-Iglesias, P. Spencer, E. Clarke, R. Murray, and A. Miller, *Electron. Lett.* **43**, 686 (2007).

<sup>7</sup>T. Piwonski, J. Pulka, G. Madden, G. Huyet, J. Houlihan, E. A. Viktorov, T. Erneux, and P. Mandel, *Appl. Phys. Lett.* **94**, 123504 (2009).

<sup>8</sup>T. Piwonski, I. O'Driscoll, J. Houlihan, G. Huyet, R. Manning, and A. Uskov, *Appl. Phys. Lett.* **90**, 122108 (2007).

<sup>9</sup>H. Haug and A.-P. Jauho, *Quantum Kinetics in Transport and Optics of Semiconductors*, Springer Series in Solid-State Sciences Vol. 123 (Springer, Berlin, 2008).

<sup>10</sup>H. Yokoyama, *IEICE Trans. Electron.* **E85**, 27 (2002).

<sup>11</sup>J. Mulet and J. Mork, *IEEE J. Quantum Electron.* **42**, 249 (2006).

<sup>12</sup>G. Vincent, A. Chantre, and D. Bois, *J. Appl. Phys.* **50**, 5484 (1979).